ORIGINAL ARTICLE

Pathogenicity evaluation and the genotype–phenotype analysis of *OPA1* variants

Xingyu Xu[1] · Panfeng Wang[1] · Xiaoyun Jia[1] · Wenmin Sun[1] · Shiqiang Li[1] · Xueshan Xiao[1] · J. Fielding Hejtmancik[2] · Qingjiong Zhang[1]

Abstract

Autosomal dominant optic atrophy (ADOA) is an important cause of irreversible visual impairment in children and adolescents. About 60–90% of ADOA is caused by the pathogenic variants of *OPA1* gene. By evaluating the pathogenicity of *OPA1* variants and summarizing the relationship between the genotype and phenotype, this study aimed to provide a reference for clinical genetic test involving *OPA1*. Variants in *OPA1* were selected from the exome sequencing results in 7092 cases of hereditary eye diseases and control groups from our in-house data. At the same time, the urine cells of some optic atrophy patients with *OPA1* variants as well as their family members were collected and oxygen consumption rates (OCR) were measured in these cells to evaluate the pathogenicity of variants. As a result, 97 variants were detected, including 94 rare variants and 3 polymorphisms. And the 94 rare variants were classified into three groups: pathogenic (33), variants of uncertain significance (19), and likely benign (42). Our results indicated that the frameshift variants at the 3′ terminus might be pathogenic, while the variants in exon 7 and intron 4 might be benign. The penetrance of the missense variants was higher than that of truncation variants. The OCR of cells with pathogenic *OPA1* variants were significantly lower than those without pathogenic variants. In conclusion, some variants might be benign although predicted pathogenic in previous studies while some might have unknown pathogenesis. Measuring the OCR in urine cells could be used as a method to evaluate the pathogenicity of some *OPA1* variants.

Keywords Autosomal dominant optic atrophy · *OPA1* · Variant · Pathogenicity

Introduction

The *OPA1* gene encodes a protein that localizes to the inner mitochondrial membrane and regulates several important cellular processes, including those that stabilize the mitochondrial network, regulate oxidative phosphorylation, and confer protection from apoptosis by preventing cytochrome c oxidase release (Olichon et al. 2002; Frezza et al. 2006; Zanna et al. 2008; Varanita et al. 2015; Liu and Chan 2017).

Pathogenic variants in *OPA1* cause optic atrophy 1 (OMIM 165500), the most common form of autosomal dominant optic atrophy, affecting 1:10,000 to 1:40,000 people in the general population (Cohn et al. 2007; Yu-Wai-Man et al. 2010a; Almind et al. 2012). With the application of next-generation sequencing, a growing number of *OPA1* variants was detected. Interpreting the pathogenicity of these variants remains challenging. Therefore, a systematic analysis of the relationship between the *OPA1* genotype and phenotype as well as some function studies may be of significant benefit for both clinical and research efforts.

There are 31 exons in *OPA1*, namely exon 1 to 29, exon 4b, and exon 5b. Among them, exon 29 is non-protein-coding. The alternate splice patterns in exon 4, exon 4b and exon 5b result in 8 transcript isoforms (Fig. 1).

The eight isoforms are ubiquitously expressed but differ in amount depending on the tissues and organs. In human retina, the expression levels of transcripts containing 4b and 5b are relatively low, while consist mainly of the isoform

✉ Qingjiong Zhang
zhangqji@mail.sysu.edu.cn; zhangqingjiong@gzzoc.com

1   State Key Laboratory of Ophthalmology, Pediatric and Genetic Eye Clinic, Zhongshan Ophthalmic Center, Sun Yat-sen University, 54 Xianlie Road, Guangzhou 510060, China

2   Ophthalmic Genetics and Visual Function Branch, National Eye Institute, National Institutes of Health, Bethesda, MD, USA

Fig. 1 A schematic of transcript variants of *OPA1*. The transcript isoform 1 (NM_015560.2) is the original and most frequently used while the transcript isoform 8 (NM_130837.2) is the longest and the most complete, which contains 31 exons with 2 additional exons of 4b and 5b compared to transcript variant 1

1 (NM_015560.2) (Delettre et al. 2001). Most variants are described in the transcript isoform 1 and this transcript is originally identified and most frequently used.

After the precursor proteins are imported through the outer mitochondrial membrane and inner mitochondrial membrane by translocases, the membrane-anchored OPA1 long forms are generated. Afterwards, the isoforms containing the exon 4b are totally processed into the soluble short forms in the mitochondrial intermembrane space. Long forms mainly involve in mitochondria fusion whereas short forms are more essential in energetics. Thus, the completeness of OPA1 isoforms is necessary for mitochondria under different circumstances (Del Dotto et al. 2017).

As of October 2020, 567 unique *OPA1* variants were reported to cause ADOA or related diseases in *OPA1* locus-specific database (https://databases.lovd.nl/shared/genes/OPA1) supported by the Leiden Open Variation Database v.3.0 (LOVD) (Fokkema et al. 2011; Le Roux et al. 2019). The majority of *OPA1* variants are truncation variants, including nonsense, frameshift, and splicing site variants, while 27.9% (158/567) are missense variants. However, it is difficult to know whether a variant is pathogenic by in silico analysis alone, especially for isolated cases or for families with incomplete penetrance. Besides, the predicted results are sometimes unable to explain the clinical variations among patients. Therefore, a systematical analysis and summary of underlying *OPA1* genotype–phenotype correlations is expected both in clinical genetics and follow-up studies.

In this study, variants of *OPA1* were selected from 7092 probands with hereditary eye diseases and control groups who underwent whole exome sequencing (WES) or targeted exome sequencing (TES). In total, 97 variants were identified including 94 rare variants and 3 polymorphic variants. Among them, 33 variants were pathogenic while 8 pathogenic variants were novel. Detailed phenotypic analysis and family cosegregation were performed in the 36 families with pathogenic *OPA1* variants. In addition, all variants from the

published literature as well as those in *OPA1* locus-specific database were reevaluated. Unexpectedly, some variants including missense and truncation variants might be benign although previously reported to be damaging. In the meantime, measurements of the oxygen consumption rates (OCR) of urine cells were applied to provide a noninvasive and alternative way to evaluate the pathogenicity of *OPA1* variants, which might be useful in addition to conventional online bioinformatics analyses. The results in this study may be of assistance not only for *OPA1* alone but also for some other genes in autosomal dominant inheritance. And this study suggests that a detailed and systematical evaluation for a specific gene is valuable especially when genetic tests are more and more commonly applied in the clinical applications.

Materials and methods

Patient recruitment

Patients and their family members with *OPA1* variants as well as control groups were recruited from the Pediatric and Genetic Clinic of the Zhongshan Ophthalmic Center (ZOC). All patients underwent routine ophthalmological examination, and selected patients had fundus photograph, electroretinogram, and optical coherence tomography. The study conformed to the tenets of the Helsinki Declaration, and was approved by the ZOC institutional review board. Written informed consent was obtained from all participants or their guardians prior to the collection of clinical data, venous blood and urine samples.

Variant acquisition

Variants in *OPA1* were selected from the exome sequencing results in 7092 cases which consisted of 298 cases who

suffered from optic atrophy, 6302 cases of other hereditary eye diseases (including inherited retinal dystrophy, early-onset high myopia, familial exudative vitreoretinopathy et al.) as well as 492 normal controls from our in-house data. The variants in nuclear DNA were detected using whole exome sequencing or targeted exome sequencing as we previously described (Wang et al. 2019; Li et al. 2020). The targeted exome sequencing was based on the custom-designed ophthalmic targeted sequencing panel that targets 126 genes commonly detected in Chinese families with different forms of hereditary eye diseases. These genes including *OPA1* accounted for more than 95% of the causative genes detected in our previously analyzed cases (Jiang et al. 2014; Xu et al. 2015, 2016). On the other hand, variants in mitochondrial DNA were directly detected by Sanger sequencing.

Variant nomenclature

OPA1 variants were described according to the transcript isoform 8 (accession number NM_130837.2) which representing the longest transcript contains two additional exons of 4b and 5b compared to the transcript isoform 1 (NM_015560.2). Since exon 4b and 5b were referred to isoform 1, the coding exons were named 1–30, instead of 1–4, 4b, 5, 5b, and 6–28. The nomenclature was in accordance with the recommendations of the Human Genome Variation Society (HGVS, version 2.0, http://varnomen.hgvs.org) (den Dunnen et al. 2016).

Variant evaluation

Variants detected in *OPA1* by exome sequencing were initially filtered as described in our former studies (Jiang et al. 2014). All candidate pathogenic variants were confirmed by Sanger sequencing. The consequences of missense variants were predicted by PolyPhen-2 (http://genetics.bwh.harvard.edu/pph2/), SIFT (http://sift.jcvi.org), PROVEAN (http://provean.jcvi.org/genome_submit_2.php), Combined Annotation-Dependent Depletion (CADD, https://cadd.gs.washington.edu/, version 1.4) and Rare Exome Variant Ensemble Learner (REVEL, https://sites.google.com/site/revelgenomics/). Afterwards, to make the predictions specific, the scores of CADD and REVEL for every *OPA1* missense variant in the Genome Aggregation Database (gnomAD, https://gnomad.broadinstitute.org) were obtained. The weighted percentiles were then calculated based on the scores and allele numbers. The percentiles of 90% were applied as cut-off scores between pathogenicity and non-pathogenicity (26.4 in CADD and 0.817 in REVEL). A missense variant was regarded as computationally pathogenic if deleterious predictions came from no less than four types of online tools accordingly. Every variant that could potentially affect a splice site was evaluated by Berkeley Drosophila Genome Project splice site prediction (BDGP, http://www.fruitfly.org/seq_tools/splice.html) and Human Splicing Finder (HSF, http://www.umd.be/HSF3/HSF.html). Through analysis of bioinformatics prediction, gnomAD allele frequency comparison, genotype–phenotype, cosegregation and previous studies, combined with the ACMG (American College of Medical Genetics and Genomics) standards (Richards et al. 2015), the pathogenicity of *OPA1* variants was classified and the phenotypes of patients with pathogenic *OPA1* variants were evaluated.

A variant was identified as pathogenic when the following criteria were met: (1) a truncation variant detected in ADOA patients, (2) a missense variant detected in ADOA patients with computationally pathogenic predictions. While a variant detected in non-ADOA patients with pathogenic predictions was regarded as VUS (variant of uncertain significance). And the rest were considered as likely benign.

Review of reported *OPA1* variants

The reported *OPA1* variants were searched in the PubMed (https://pubmed.ncbi.nlm.nih.gov/) and the *OPA1* locus-specific database (https://databases.lovd.nl/shared/genes/OPA1) (Fokkema et al. 2011; Le Roux et al. 2019) until October 2020 with "*OPA1*" as the key word. The frequency, pathogenicity and potential genotype–phenotype correlations were summarized based on data from PubMed.

Isolation and culture of human urine cells

Sterilized containers were used for mid-stream urine collection as previously described (Dorrenhaus et al. 2000). Exfoliated cells were centrifuged and washed with PBS (Thermo Fisher Scientific, Waltham, MA, USA) containing 1% penicillin–streptomycin (Thermo Fisher Scientific). The cells were then suspended with REGM (Renal Epithelial Cell Growth Medium) (Lonza, Basel, Switzerland) before being transferred to 6-well plates coated with 1% Matrigel (Corning, Corning, NY, USA) and cultured in an incubator with 37 °C and 5% CO_2. The medium was replaced every other day. Visible cell colonies appeared routinely after 5–7 days. The urine cells were passaged by addition of 0.25% trypsin (Thermo Fisher Scientific) containing 1 mM EDTA when the cell density reached an 80–90% confluence, usually in less than 3 weeks.

Measurement of mitochondrial respiration parameters

An Agilent Seahorse XF Cell Mito Stress Test Kit (Agilent, Wilmington, DE, USA) was applied to analyze mitochondrial function by measuring the oxygen consumption rates (OCR) with a Seahorse XF24 Flux Analyzer (Seahorse

Bioscience, Billerica, MA, USA). 8×10^4 cells were seeded in 24-well culture microplates in REGM medium (Lonza) 24 h prior to the assay to achieve an adherent monocellular layer no less than 90% confluence based on our preliminary experiments. Cells were applied after the second passage to insure their viability. The assay medium was prepared by supplementing Seahorse XF DMEM medium with 1 mM pyruvate, 2 mM glutamine, and 10 mM glucose, warmed to 37 °C, and adjusted pH to 7.4. Solutions of 1.5 µM oligomycin, 2.0 µM FCCP (Carbonyl cyanide-4 [trifluoromethoxy] phenylhydrazone), 0.5 µM Rot/AA (Rotenone, and Antimycin A) were loaded into the sensor cartridge in ports A, B, and C successively as per the manufacturer's instructions. OCR measurements were initiated every 8 min, resulting in 3 measurements in each stage. All the measurements were completed in approximately 95 min. The calculations used in this test were demonstrated as follows: basal respiration = (measurement prior to injection of oligomycin) − (measurement after injection of Rot/AA); ATP production = (measurement prior to injection of oligomycin) − (measurement after injection of oligomycin); spare respiratory capacity = (maximum respiration) − (basal respiration). Since the samples were measured in six different batches, cells from a control without known pathogenic variants related to mitochondria were applied in every batch to normalize all the data to reduce variabilities between microplates as many as possible. Normalization was performed according to protein content of the normal control in every batch as the manufacturer guided (Divakaruni et al. 2014). Measurements of the normal control were baselined to the same parameter values via the instrument software, other measurements were shifted proportionally to make them comparable.

Statistical analysis

Data were reported in means ± standard deviation. Statistical significance was evaluated by one-way analysis of variance (ANOVA) among the groups using SPSS 21.0 (IBM, Armonk, NY, USA). The minimum level of significance was set at $P < 0.05$. Multiple comparisons tests were made between groups with the method of Bonferroni.

Results

OPA1 variants in probands

A total of 97 variants were detected from 7092 probands with hereditary eye diseases and control groups, including 94 rare variants and 3 polymorphic variants. These 94 rare variants consisted of 68 missense variants, 4 nonsense variants, 16 splicing variants, 5 frameshift deletions, and

1 in-frame deletion. Notably, 3 variants including 2 missense variants and 1 in-frame deletion were detected in exon 7 which was absent in transcript isoform 1 (Table 1). The pathogenicity of 94 rare variants was evaluated based on the phenotypes of probands, bioinformatic predictions, frequencies in gnomAD database, family cosegregation and previous reports under the standards of ACMG. As a result, 33 were pathogenic, 19 were variants of uncertain significance and 42 were likely benign. 33 pathogenic variants, including 8 novels, were detected in 36 families. Most of these pathogenic variants were truncation variants (60.6%, 20/33), the rest were missense variants distributed mainly in the GTPase domain (61.5%, 8/13). Particularly, the splicing variant of c.556 + 2 T > G in intron 4 might be benign although it had very strong evidence of pathogenicity according to ACMG standards. And the in-frame deletion of c.712_714del in exon 7 might be benign as well (Fig. 2a, Table 1).

Phenotypes of patients with pathogenic *OPA1* variants in 36 families

There were 36 probands from 36 families with pathogenic variants. 34 were diagnosed with ADOA, 1 with optic atrophy in autosomal recessive inheritance and 1 suffered from LCA-like oculopathy. The ages of onset of ADOA probands ranged from 2 to 27 (9.7 ± 5.7, mean ± SD). The ADOA probands complained of visual impairment without self-reported hearing loss or other neurological complications. No significant correlations were observed between visual impairment and different sex or variant types. In the ADOA family, the penetrance of truncation variants was 82.9% (34/41) while the penetrance of missense variants was 97.1% (33/34) (Fig. 3, Table 2, Supplementary figures).

Frequency and genotype–phenotype correlations of *OPA1* variants in literature

As of October 2020, about 567 *OPA1* variants were listed in the *OPA1* locus-specific database, of which most were truncation variants (61.3%, 358/567). Of the 567, 406 *OPA1* variants were reported in the PubMed. Most variants were truncation variants (62.8%, 255/406) and the vast majority of variants (97.0%, 394/406) were detected in patients with optic atrophy including ADOA, optic atrophy plus syndrome and Behr syndrome (Fig. 2b, Supplementary table). Optic atrophy plus syndrome was more common in patients with missense variants than those with truncation variants, while those with gross insertions or deletions manifested as ADOA without other neurological complications conformed to cosegregation.

Table 1 OPA1 variants identified in this study

No	Position	DNA change	RNA change	Protein	CADD	REVEL	Poly-phen2	SIFT	PROVEAN	BDGP	HSF	gnomAD AF	Proband No	Diagnosis§	ACMG	References
Pathogenic																
1	Exon 2	c.60_61del	r.?	p.(His20Glnfs*52)	–	–	–	–	–	–	–	–	1	ADOA	P	LSD OPA1_000604
2	Exon 2	c.112C>T	r.?	p.(Arg38*)	38	–	–	–	–	–	–	–	1	ADOA	P	Thiselton et al. (2002)
3	Exon 3	c.356 T>C	r.?	p.(Phe119Ser)	24.6	0.622	B	D	D	–	–	–	1	Other	VUS	LSD OPA1_000605
4	Exon 3	c.380C>T	r.?	p.(Pro127Leu)	28.5	0.824	PRD	D	D	–	–	0.00002122	1	ADOA	VUS	LSD OPA1_000389
5	Intron 9	c.949-2A>C	r.spl?	p.(?)	29.6	–	–	–	–	NSSC	SSC	–	1	ADOA	P	Chen et al. (2013)
6	Exon 10	c.1034G>A	r.?	p.(Arg345Gln)	29.3	0.867	D	D	D	–	–	–	2	ADOA	LP	Delettre et al. (2000)
7	Intron 10	c.1035+1G>A	r.spl?	p.(?)	26.2	–	–	–	–	SSC	NSSC	–	1	ADOA	P	Chen et al. (2014)
8	Intron 11	c.1149+1G>A	r.spl?	p.(?)	31	–	–	–	–	SSC	NSSC	–	1	ADOA	P	LSD OPA1_000310
9	Intron 11	c.1150-1G>C	r.spl?	p.(?)	34	–	–	–	–	SSC	NSSC	–	1	ADOA	P	LSD OPA1_000608
10	Exon 14	c.1306A>T	r.?	p.(Thr436Ser)	27.6	0.783	PRD	D	N	–	–	–	1	ADOA	LP	Li et al. (2017)
11	Exon 14	c.1337 T>G	r.?	p.(Leu446Arg)	29.2	0.84	PRD	D	D	–	–	–	1	ADOA	P	Zhang et al. (2017)
12	Exon 14	c.1349 T>G	r.?	p.(Val450Gly)	27.8	0.984	D	D	D	–	–	–	1	ADOA	LP	Li et al. (2017)
13	Intron 14	c.1377+1G>A	r.spl?	p.(?)	34	–	–	–	–	SSC	NSSC	–	1	ADOA	P	Delettre et al. (2001)
14	Intron 14	c.1377+2dup	r.spl?	p.(?)	34	–	–	–	–	SSC	SSC	–	1	ADOA	P	LSD OPA1_000354
15	Intron 14	c.1377+5G>C	r.spl?	p.(?)	22.3	–	–	–	–	NSSC	NSSC	–	1	ADOA	VUS	Zhang et al. (2017)
16	Exon 15	c.1442 T>A	r.?	p.(Met481Lys)	27.3	0.951	PRD	D	D	–	–	–	1	ADOA	LP	LSD OPA1_000610
17	Exon 15	c.1454_1470del	r.?	p.(Ala486Serfs*8)	–	–	–	–	–	–	–	–	1	ADOA	P	LSD OPA1_000611
18	Exon 16	c.1478A>G	r.?	p.(Asp493Gly)	34	0.969	D	D	D	–	–	–	2	ADOA	P	Dadgar et al. (2006)
19	Exon 16	c.1481G>T	r.?	p.(Gly494Val)	29.2	0.929	D	D	D	–	–	–	1	ADOA	LP	Morny et al. (2015)
20	Exon 16	c.1567A>G	r.?	p.(Lys523Glu)	29.1	0.977	D	D	D	–	–	–	1	ADOA	LP	Pesch et al. (2001)
21	Exon 18	c.1734del	r.?	p.(Gln579Argfs*6)	–	–	–	–	–	–	–	–	1	ADOA	P	LSD OPA1_000499
22	Exon 20	c.1934G>A	r.spl?	p.(Arg645Gln); p.(?)	34	0.898	PRD	D	D	SSC	SSC	0.00003538	3	ADOA+Other	P	Chen et al. (2014)
23	Exon 23	c.2284G>T	r.?	p.(Glu762*)	43	–	–	–	–	–	–	–	1	ADOA	P	Chen et al. (2014)

Table 1 (continued)

No	Position	DNA change	RNA change	Protein	CADD	REVEL	Poly-phen2	SIFT	PROVEAN	BDGP	HSF	gnomAD AF	Proband No	Diagnosis§	ACMG	References
24	Exon 25	c.2519A>G	r.?	p.(Gln840Arg)	34	0.935	PSD	D	D	–	–	–	1	ADOA	VUS	Schimpf et al. (2008)
25	Exon 26	c.2470C>T	r.?	p.(Arg824*)	40	–		–	–	–	–	–	1	ADOA	P	Yoshida et al. (2006)
26	Exon 26	c.2661G>A	r.spl?	p.(=); p.(?)	22.4	–		–	–	SSC	SSC	–	1	ADOA	P	Almind et al. (2012)
27	Intron 26	c.2661+3A>C	r.spl?	p.(?)	20.5	–		–	–	SSC	SSC	–	1	ADOA	P	LSD OPA1_000612
28	Exon 27	c.2734C>T	r.?	p.(Arg912*)	41	–		–	–	–	–	–	2	ADOA	P	Ferre et al. (2009)
29	Exon 28	c.2810G>A	r.?	p.(Arg937His)	33	0.83	PRD	D	D	–	–	–	1	ADOA	LP	LSD OPA1_000607
30	Exon 29	c.2873_2876del	r.?	p.(Val958Glyfs*3)	–	–		–	–	–	–	–	2	ADOA+Other	P	Ferre et al. (2009)
31	Intron 29	c.2983+5G>A	r.spl?	p.(?)	16.51	–		–	–	SSC	SSC	–	1	ADOA	LP	Schimpf et al. (2008)
32	Intron 29	c.2983+6T>C	r.spl?	p.(?)	15.07	–		–	–	SSC	SSC	–	1	ADOA	LP	Ferre et al. (2009)
33	Exon 30	c.3020del	r.?	p.(Phe1007Serfs*16)	–	–		–	–	–	–	–	1	ADOA	P	LSD OPA1_000499
Variants of uncertain significance																
34	Exon 2	c.305A>G	r.?	p.(Tyr102Cys)	26.2	0.889	D	D	D	–	–	0.00002009	1	Other	VUS	Ferre et al. (2009)
35	Exon 2	c.320C>T	r.?	p.(Ser107Leu)	26.4	0.699	PRD	D	D	–	–	0.00001071	1	Other	VUS	–
36	Exon 2	c.331G>A	r.?	p.(Gly111Ser)	27	0.894	PSD	T	D	–	–	–	1	Other	VUS	–
37	Intron 4	c.556+2T>G	r.spl?	p.(?)	34	–		–	–	SSC	SSC	0.00001998	2	Other	VUS	Zhang et al. (2017)
38	Exon 11	c.1061C>G	r.?	p.(Ala354Gly)	26.1	0.885	PSD	D	D	–	–	–	1	Other	VUS	–
39	Exon 12	c.1202G>C	r.?	p.(Arg401Pro)	32	0.921	D	D	D	–	–	–	1	Other	VUS	–
40	Exon 13	c.1234G>A	r.?	p.(Ala412Thr)	27.5	0.836	D	D	N	–	–	0.00003190	4	ADOA+Other	VUS	Ferre et al. (2009)
41	Exon 15	c.1379C>T	r.?	p.(Thr460Ile)	34	0.815	PRD	D	D	–	–	–	1	Other	VUS	–
42	Exon 15	c.1397C>G	r.?	p.(Ala466Gly)	32	0.747	D	D	D	–	–	0.00000398	2	Other	VUS	–
43	Exon 16	c.1583A>G	r.?	p.(Glu528Gly)	32	0.878	PSD	D	D	–	–	–	1	Other	VUS	–
44	Exon 16	c.1586A>T	r.?	p.(Lys529Ile)	27.1	0.826	PSD	D	D	–	–	–	1	Other	VUS	–
45	Exon 18	c.1732T>A	r.?	p.(Phe578Ile)	28	0.929	PRD	D	D	–	–	–	1	Other	VUS	Chen et al. (2014)
46	Exon 19	c.1804G>A	r.?	p.(Ala602Thr)	29.8	0.696	PRD	D	D	–	–	–	1	Other	VUS	–
47	Exon 22	c.2014G>C	r.?	p.(Glu672Gln)	34	0.65	PRD	D	D	–	–	–	1	Other	VUS	–
48	Exon 22	c.2087C>T	r.?	p.(Ala696Val)	28.8	0.747	PRD	D	D	–	–	0.00000398	1	Other	VUS	–
49	Exon 23	c.2318C>T	r.?	p.(Ala773Val)	32	0.797	PSD	D	D	–	–	–	1	Other	VUS	Chen et al. (2014)

Table 1 (continued)

No	Position	DNA change	RNA change	Protein	CADD	REVEL	Poly-phen2	SIFT	PROVEAN	BDGP	HSF	gnomAD AF	Proband No	Diagnosis§	ACMG	References
50	Exon 29	c.2959C>T	r.?	p.(Arg987Cys)	26.7	0.855	D	D	D	–	–	0.00001768	1	Other	VUS	Nochez et al. (2009)
51	Exon 29	c.2960G>A	r.?	p.(Arg987His)	32	0.83	PRD	D	D	–	–	–	1	Other	VUS	–
52	Exon 30	c.3031C>T	r.?	p.(Leu1011Phe)	27.8	0.785	PRD	D	D	–	–	–	1	Other	VUS	–
Likely benign																
53	Exon 1	c.23C>T	r.?	p.(Ala8Val)	23.6	0.376	B	T	N	–	–	–	1	Other	VUS	–
54	Exon 2	c.71T>C	r.?	p.(Ile24Thr)	16.23	0.295	B	T	N	–	–	–	1	Other	VUS	–
55	Exon 2	c.113G>A	r.?	p.(Arg38Gln)	24.6	0.399	B	D	N	–	–	–	1	Other	VUS	–
56	Exon 2	c.131A>G	r.?	p.(His44Arg)	10.86	0.222	B	D	N	–	–	0.00000402	1	Other	VUS	–
57	Exon 2	c.188C>T	r.?	p.(Ser63Phe)	24.7	0.546	B	D	N	–	–	–	1	Other	VUS	–
58	Exon 2	c.205C>T	r.?	p.(Pro69Ser)	19.31	0.231	B	T	N	–	–	–	2	Other	VUS	–
59	Exon 2	c.275G>C	r.?	p.(Arg92Thr)	24.1	0.694	B	D	N	–	–	–	1	Other	VUS	Sun et al. (2015)
60	Exon 2	c.326T>C	r.?	p.(Val109Ala)	25.8	0.807	B	D	D	–	–	0.00002017	1	Other	VUS	–
61	Exon 3	c.430G>A	r.?	p.(Asp144Asn)	22.7	0.267	B	T	D	–	–	0.00003186	1	Other	LB	–
62	Exon 3	c.442G>C	r.?	p.(Asp148His)	27.6	0.715	PSD	D	N	–	–	–	1	Other	VUS	–
63	Exon 6	c.619G>A	r.?	p.(Glu207Lys)	17.45	0.315	B	T	N	–	–	0.00009149	14	Other	VUS	Zhang et al. (2017)
64	Exon 6	c.647G>A	r.?	p.(Arg216His)	11.09	0.261	B	T	N	–	–	0.00002784	2	Other	VUS	–
65	Exon 7	c.704T>C	r.?	p.(Leu235Ser)	22.9	0.342	B	T	N	–	–	0.00001989	2	Other	VUS	–
66	Exon 7	c.712_714del	r.?	p.(Gln238del)	–	–	–	–	–	–	–	–	3	Other	VUS	–
67	Exon 7	c.785G>C	r.?	p.(Arg262Pro)	24.1	0.546	B	D	N	–	–	–	2	Other	VUS	–
68	Exon 13	c.1294G>A	r.?	p.(Val432Ile)	24.8	0.659	B	T	N	–	–	0.00001594	3	Other	VUS	Chen et al. (2014)
69	Intron 13	c.1306-9C>T	r.spl?	p.(?)	8.143	–	–	–	–	NSSC	SSC	0.00003200	1	Other	VUS	–
70	Intron 14	c.1377+9A>G	r.spl?	p.(?)	12.1	–	–	–	–	NSSC	SSC	0.00003589	1	Other	VUS	–
71	Exon 16	c.1555T>C	r.?	p.(Phe519Leu)	25.2	0.891	PRD	T	D	–	–	0.00000796	1	Other	VUS	Zhang et al. (2017)
72	Exon 17	c.1630A>G	r.?	p.(Lys544Glu)	24.7	0.72	PSD	T	D	–	–	0.00001198	2	Other	VUS	–
73	Exon 18	c.1552T>C	r.?	p.(Tyr518His)	24.5	0.69	B	D	D	–	–	–	1	Other	VUS	–
74	Exon 19	c.1835G>A	r.?	p.(Arg612Gln)	28.8	0.793	B	T	D	–	–	–	1	Other	VUS	–
75	Exon 22	c.2054C>T	r.?	p.(Thr685Ile)	23.3	0.76	PSD	T	D	–	–	–	1	Other	VUS	–
76	Exon 22	c.2080C>G	r.?	p.(Pro694Ala)	25.6	0.764	PRD	T	D	–	–	–	1	Other	VUS	–
77	Exon 22	c.2173G>A	r.?	p.(Val725Ile)	22.5	0.374	B	T	N	–	–	–	1	Other	VUS	–
78	Exon 23	c.2212C>T	r.?	p.(Arg738Cys)	25	0.581	B	T	D	–	–	–	3	Other	VUS	–
79	Exon 23	c.2213G>A	r.?	p.(Arg738His)	24	0.649	PSD	T	N	–	–	0.00003187	2	Other	VUS	Zhou et al. (2018)
80	Exon 23	c.2248G>A	r.?	p.(Asp750Asn)	23.8	0.417	PSD	T	N	–	–	–	1	Other	VUS	–
81	Exon 23	c.2275G>A	r.?	p.(Val759Ile)	25.2	0.709	PRD	D	N	–	–	–	1	Other	VUS	–
82	Exon 24	c.2334G>C	r.?	p.(Arg778Ser)	24.4	0.781	PSD	D	D	–	–	–	1	Other	VUS	–
83	Intron 24	c.2441-4C>T	r.spl?	p.(?)	13.1	–	–	–	–	NSSC	NSSC	–	1	Other	VUS	–

Table 1 (continued)

No	Position	DNA change	RNA change	Protein	Poly-phen2	REVEL	CADD	SIFT	PROVEAN	BDGP	HSF	gnomAD AF	Proband No	Diagnosis§	ACMG	References
84	Exon 25	c.2464G>A	r.?	p.(Val822Met)	B	0.259	15.67	T	N	–	–	–	1	Other	VUS	–
85	Exon 25	c.2480A>G	r.?	p.(Lys827Arg)	B	0.262	22.4	T	N	–	–	0.00000712	3	Other	VUS	–
86	Exon 25	c.2483A>G	r.?	p.(Lys828Arg)	B	0.266	23.2	T	N	–	–	–	1	Other	VUS	–
87	Exon 26	c.2544 T>A	r.?	p.(Asn848Lys)	B	0.297	18.53	T	D	–	–	0.00004782	4	Other	VUS	–
88	Exon 26	c.2471G>A	r.?	p.(Arg824Gln)	B	0.396	23.9	T	N	–	–	0.00005176	1	Other	VUS	–
89	Exon 26	c.2545G>A	r.?	p.(Ala849Thr)	PRD	0.765	25.5	T	N	–	–	–	1	Other	VUS	–
90	Exon 26	c.2717A>G	r.?	p.(Asn906Ser)	B	0.132	14.6	T	N	–	–	–	1	Other	VUS	–
91	Exon 27	c.2723G>C	r.?	p.(Cys908Ser)	B	0.522	23.3	T	D	–	–	–	1	Other	VUS	–
92	Exon 27	c.2735G>A	r.?	p.(Arg912Gln)	B	0.43	23.8	T	N	–	–	–	1	Other	VUS	–
93	Exon 28	c.2814A>G	r.?	p.(Ile938Met)	B	0.733	24.6	T	N	–	–	–	2	Other	VUS	–
94	Intron 29	c.2984-4A>G	r.spl?	p.(?)	–	–	7.984	–	–	NSSC	SSC	0.00049683	6	Other	VUS	–

CADD combined annotation-dependent depletion, *REVEL* rare exome variant ensemble learner, *PolyPhen2* polymorphism phenotyping version 2, *SIFT* sorting tolerant from intolerant, *PROVEAN* protein variation effect analyzer, *BDGP* Berkeley Drosophila Genome Project splice site prediction, *HSF* human splicing finder, *gnomAD AF* Allele Frequency in Genome Aggregation Database, *Proband No.* number of proband, *Diagnosis§* probands of control groups or those with hereditary eye diseases other than ADOA (such as retinitis pigmentosa, high myopia et al.) were marked as "Other", *ACMG* The American College of Medical Genetics and Genomics, *P* pathogenic, *LP* likely pathogenic, *VUS* variant of uncertain significance, *T* tolerated, *D* deleterious, *B* benign, *PSD* possibly damaging, *PRD* probably damaging, *N* neutral, *SSC* splicing site change, *NSSC* no splicing site change, *LSD* unpublished but included in OPA1 Locus-Specific Database with a database ID, – not applicable

Biallelic variants in *OPA1*

There were 5 probands with biallelic variants in this study and 21 more in former studies. The proband with homozygous variant of c.356 T > C showed typical optic atrophy while his heterozygous parents were asymptomatic. This variant might be tolerated in heterozygous status but pathogenic in homozygous status. Measurements of the OCR in urine cells were taken in this family to evaluate the pathogenicity of this variant. As with the proband of c.[305A > G]; [c.2873_2876del], he was diagnosed with LCA-like oculopathy because of poor vision and extinguished amplitudes in ERG. However, the correlation between the heavily impaired vision and these variants needed further investigations (Table 3).

Urine cells collection and OCR measurements

A total of 20 individuals from 15 families were recruited for this study (Fig. 4). They consisted of eight ADOA patients with *OPA1* variants, four patients with optic atrophy because of variants in other genes related to mitochondria, three family members without clinical symptoms, four patients with hereditary retinopathies not directly related to mitochondria, and a normal control.

Urine cell colonies from individual participants were observed 5–7 days after the isolation and subsequent culture. All the primary cells reached 80–90% confluence within 3 weeks. The cells were passaged once and used for subsequent measurements (Fig. 5).

There were four major phases simulating different physiological status during the OCR measurements, including the baseline before the injection of oligomycin, the measurements after injection of oligomycin, the measurements after injection of FCCP and the measurements after injection of Rot/AA. Basal respiration, ATP production and spare respiratory capacity could be calculated afterwards (Fig. 6a). According to the results of the calculations, the OCR could be divided into four subgroups (I, II, III, and IV). Group I data included those of the most severely reduced mitochondrial OCR in the urine cells from patients with pathogenic variants directly related to mitochondria, including two with homozygous variants in *NDUFAF5* (F01-II:1 and F01-II:2), one with m.3460G > A in *MT-ND1* (F02-II:1), one with m.11778G > A in *MT-ND4* (F03-II:1), and six with either heterozygous truncation variants or biallelic variants in *OPA1* ([c.1150-1G > C]; [=] in F04-I:2, [c.1377 + 2dup]; [=] in F05-II:1, [c.2661 + 3A > C]; [=] in F06-II:2, [c.2734C > T]; [=] in F07-II:1, c.[356 T > C]; [356 T > C] in F08-II:2, and c.[1150-1G > C]; [2814A > G] in F04-II:1), respectively. Group II data showed moderately reduced mitochondrial OCR in the urine cells from patients with heterozygous missense variants in *OPA1*

Fig. 2　a The distribution and frequency of *OPA1* variants identified in this study are shown in the mRNA sequence (Ref. NM_015560.2). The position and frequency of pathogenic variants are demonstrated above the schematic diagram of the mRNA while those likely benign variants are indicated below. **b** The distribution and frequency of *OPA1* variants identified in previous studies are shown in the mRNA sequence (Ref. NM_015560.2). The position and frequency of reported truncation variants are demonstrated above the schematic diagram of the mRNA while those missense variants and in-frame insertions/deletions are indicated below. The domains and exons are shown in the figure except for exon 31. This exon is omitted because it is noncoding, and no potential pathogenic variants are discovered in this exon so far. The domain sequences are represented below the exons. The domain which involves the cleavage of precursor protein is marked as yellow areas
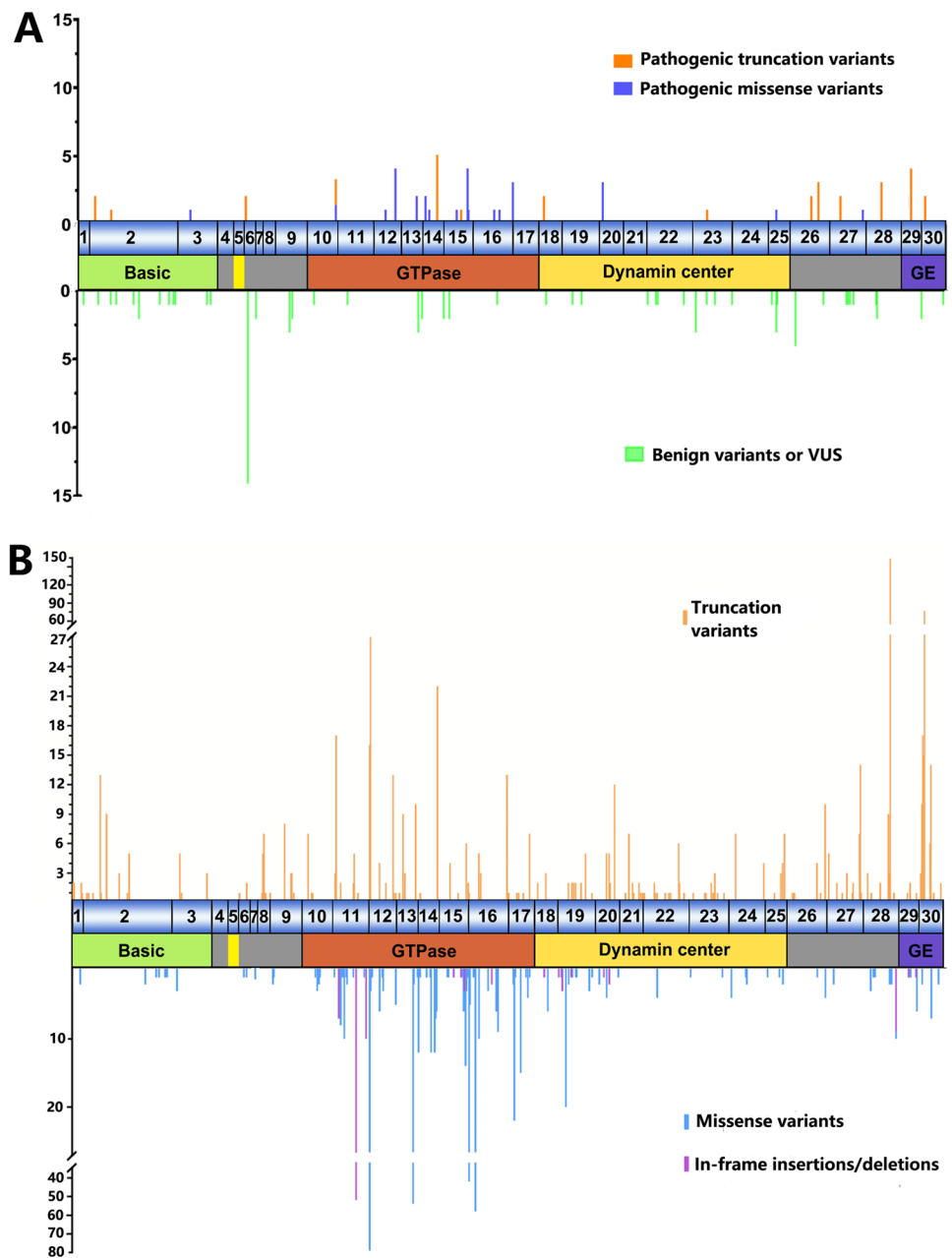
that were predicted to be pathogenic ([c.1337 T > G]; [=] in F09-I:2 and [c.1478A > G]; [=] in F10-II:1). Group III data showed normal OCR at basal respiration and ATP production but reduced OCR under stress (spare respiratory capacity) and included data from three asymptomatic carriers, including two with *OPA1* missense variants predicted to be benign ([c.356 T > C]; [=] in F08-I:1 and [c.2814A > G]; [=] in F04-I:1) and one with a heterozygous variant in *NDUFAF5* ([c.836 T > G]; [=] in F01-I:1). Group IV data consisted of those from urine cells with a normal OCR obtained from a normal control (NC) and four patients with variants in genes not directly involved in mitochondrial metabolism, including one patient with

Leber congenital amaurosis due to a homozygous variant in *SPATA7* (c.[644_647del];[644_647del]), one patient with type I ocular albinism due to a hemizygous variant in *GPR143* ([c.251-3 T > C]; [0]), one patient with retinitis pigmentosa due to a hemizygous variant in *RPGR* ([c.748 T > C]; [0]), and one patient with early-onset retinal degeneration due to biallelic variants in *RPE65* (c.[190C > G]; [200 T > G]) (Fig. 6b).

The cells from the 12 patients represented in data group I and group II, with optic atrophy, showed a significant reduction in OCR. The mean values of basal respiration, ATP production, and spare respiratory capacity for the group I patients were 42.2%, 30.6%, and 29.1%, respectively,
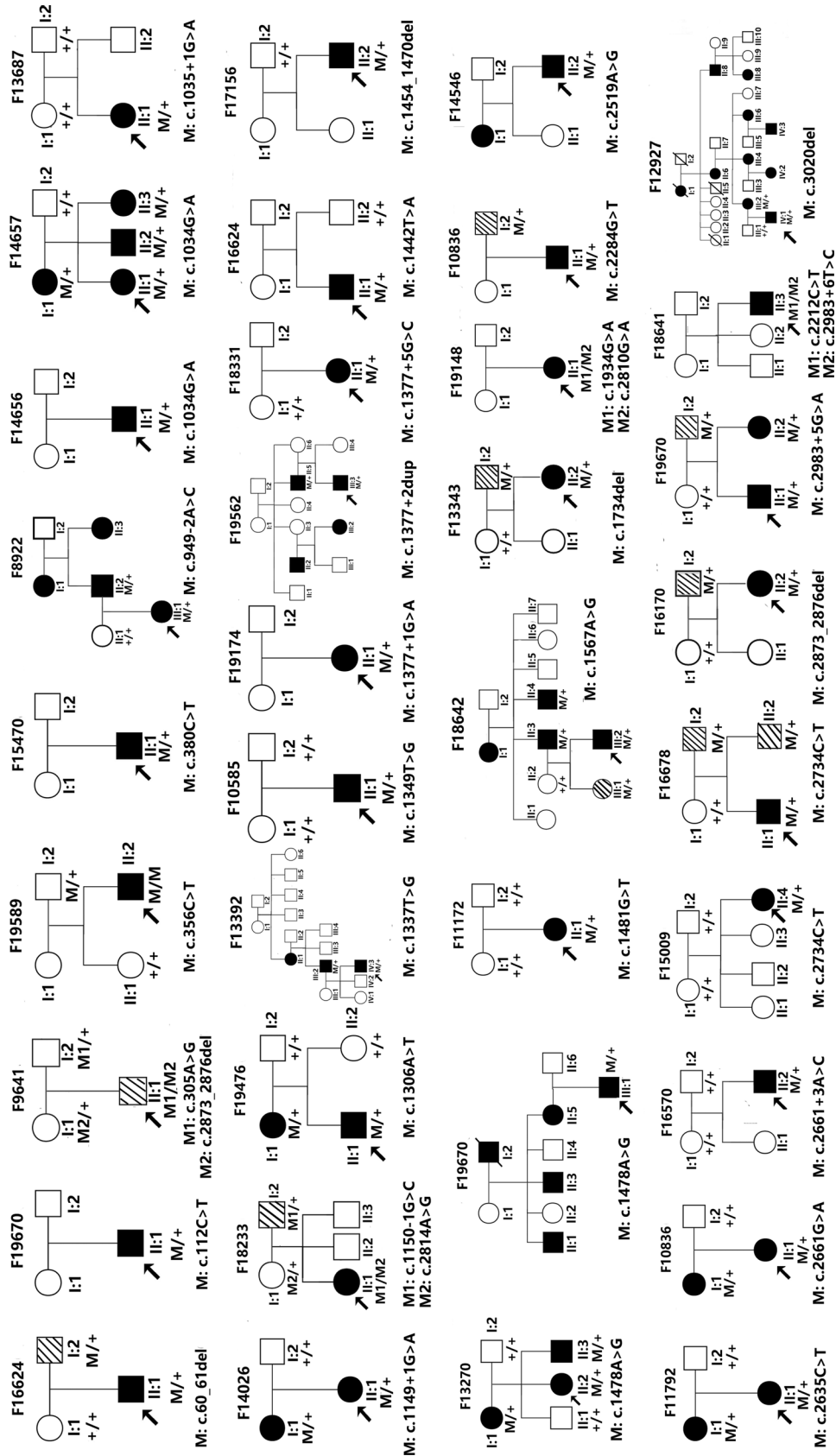
Fig. 3 The pedigrees of 36 families with pathogenic *OPA1* variants identified in this study. The proband in F9641 was diagnosed with Leber congenital amaurosis (LCA) while the proband in F19589 with autosomal recessive optic atrophy. Others manifested as ADOA

Table 2 Clinical information of ADOA probands with pathogenic *OPA1* variants

No	Nucleotide change	Protein	Sex	Age	VA OD	VA OS	Visual field defects	OCT	VEP	Brain MRI
F16624	c.60_61del	p.(His20Glnfs*52)	Male	10	0.30	0.20	NA	RNFL thinning	PL; DA	NA
F19670	c.112C>T	p.(Arg38*)	Male	7	0.40	0.50	Central and paracentral	RNFL thinning	DA	NA
F15470	c.380C>T	p.(Pro127Leu)	Male	7	0.30	0.15	NA	RNFL thinning	NA	NA
F8922	c.949-2A>C	p.(?)	Female	6	0.20	0.25	NA	RNFL thinning	PL	Normal
F14657	c.1034G>A	p.(Arg345Gln)	Female	11	0.20	0.20	NA	NA	NA	NA
F13687	c.1035+1G>A	p.(?)	Female	9	0.20	0.15	Central and paracentral	RNFL thinning	PL	Normal
F14026	c.1149+1G>A	p.(?)	Female	5	0.06	0.06	Central and paracentral	RNFL thinning	NA	NA
F18233	c.1150-1G>C	p.(?)	Female	6	0.15	0.15	NA	NA	NA	NA
	c.2814A>G	p.(Ile938Met)								
F19476	c.1306A>T	p.(Thr436Ser)	Male	7	0.60	0.60	NA	NA	NA	NA
F13392	c.1337T>G	p.(Leu446Arg)	Male	5	–	–	NA	NA	NA	NA
F10585	c.1349T>G	p.(Val450Gly)	Male	2	–	–	NA	NA	NA	NA
F19174	c.1377+1G>A	p.(?)	Female	6	0.10	0.10	Central and paracentral	RNFL thinning	NA	Normal
F19562	c.1377+2dup	p.(?)	Male	21	0.05	0.04	NA	RNFL thinning	NA	Normal
F18331	c.1377+5G>C	p.(?)	Female	9	0.25	0.20	NA	RNFL thinning	NA	NA
F16267	c.1442T>A	p.(Met481Lys)	Male	27	0.20	0.15	Central and paracentral	RNFL thinning	NA	NA
F17156	c.1454_1470del	p.(Ala486Serfs*8)	Male	13	0.60	0.60	NA	RNFL thinning	NA	Normal
F18718	c.1478A>G	p.(Asp493Gly)	Male	19	0.01	0.01	NA	RNFL thinning	NA	NA
F13272	c.1478A>G	p.(Asp493Gly)	Female	9	0.30	0.30	NA	RNFL thinning	NA	NA
F11172	c.1481G>T	p.(Gly494Val)	Female	7	0.08	0.06	NA	RNFL thinning	NA	NA
F18642	c.1567A>G	p.(Lys523Glu)	Male	6	0.20	0.10	NA	RNFL thinning	PL; DA	NA
F13343	c.1734del	p.(Gln579Argfs*6)	Female	4	–	–	NA	RNFL thinning	DA	Normal
F19148	c.1934G>A	p.(Arg645Gln)	Female	3	–	–	NA	NA	NA	NA
	c.2810G>A	p.(Arg937His)								
F11939	c.2284G>T	p.(Glu762*)	Male	7	0.30	0.40	NA	RNFL thinning	PL	NA
F14546	c.2519A>G	p.(Gln840Arg)	Male	5	–	–	NA	NA	NA	Normal
F11792	c.2635C>T	p.(Arg879*)	Female	5	0.20	0.30	NA	RNFL thinning	NA	NA
F10836	c.2661G>A	p.(=)	Female	9	0.20	0.12	NA	RNFL thinning	DA	Normal
F16570	c.2661+3A>C	p.(?)	Male	6	0.20	0.30	NA	RNFL thinning	NA	NA
F15009	c.2734C>T	p.(Arg912*)	Female	13	0.20	0.20	NA	RNFL thinning	NA	NA
F16678	c.2734C>T	p.(Arg912*)	Male	10	0.25	0.35	NA	NA	NA	NA
F16170	c.2873_2876del	p.(Val958Glyfs*3)	Female	12	0.40	0.50	NA	RNFL thinning	NA	NA
F15869	c.2983+5G>A	p.(?)	Male	20	0.12	0.12	NA	RNFL thinning	DA	NA
F18641	c.2212C>T	p.(Arg738Cys)	Male	19	0.05	0.05	Central and paracentral	RNFL thinning	DA	NA
	c.2983+6T>C	p.(?)								
F12927	c.3020del	p. (Phe1007Serfs*16)	Male	6	0.05	0.02	NA	RNFL thinning	PL	NA

VA OD visual acuity of right eye, *VA OS* visual acuity of left eye, *OCT* optical coherence tomography, *VEP* visual evoked potential, *PL* prolonged latencies, *DA* diminished amplitudes, *RNFL* retinal nerve fiber layer, *NA* not available

Table 3 Biallelic *OPA1* variants in this and previous studies

No	Status	Position	Nucleotide change	Protein	Inheritance	Phenotype	Other findings	References
1	Hom	Exon 3	c.356 T > C	p.(Phe119Ser)	AR	Optic atrophy	–	This study
2	C-het	Intron 11	c.1150-1G > C	p.(?)	AD	ADOA	–	This study
		Exon 28	c.2814A > G	p.(Ile938Met)				
3	C-het	Exon 20	c.1934G > A	p.(Arg645Gln); p.(?)	AD	ADOA	Extinguished ERG	This study
		Exon 28	c.2810G > A	p.(Arg937His)			Talipes equino-varus	
4	C-het	Exon 2	c.305A > G	p.(Tyr102Cys)	AD	LCA-like	–	This study
		Exon 29	c.2873_2876del	p.(Val958Glyfs*3)				
5	C-het	Exon 23	c.2212C > T	p.(Arg738Cys)	AD	ADOA	–	This study
		Intron 29	c.2983 + 6 T > C	p.(?)				
6	C-het	Exon 2	c.190_194del	p.(Ser64Aspfs*7)	AD	ADOA	–	Chen et al. (2013)
		Exon 13	c.1294G > A	p.(Val432Ile)				
7	C-het	Exon 10	c.937G > A	p.(Glu326Lys)	AD	ADOA	Dyschromatopsia	Pesch et al. (2001)
		Exon 10	c.1033C > T	p.(Arg345Trp)				
8	C-het	Exon 11	c.1102_1104delinsGA	p.(Ile368Glu)	AD	ADOA	–	Cohn et al. (2007)
		Exon 14	c.1337 T > G	p.(Leu446Arg)				
9	C-het	Exon 22	c.2022_2023delinsT	p.(Leu675Phefs*13)	AR	Optic atrophy	Sensorimotor disorder	Lee et al. (2016)
		Exon 29	c.2878G > A	p.(Arg959Gln)			Cataract	
10	Hom	Exon 12	c.1180G > A	p.(Ala394Thr)	AR	Spastic ataxia	Mental retardation	Rubegni et al. (2017)
11	C-het	Exon 14	c.1369G > A	p.(Val457Met)	AR	Behr syndrome	–	Amati-Bonneau et al. (2009)
		Exon 29	c.2873_2876del	p.(Val958Glyfs*3)				
12	C-het	Exon 14	c.1311A > G	p.(Ile437Met)	AR	Behr syndrome	Nystagmus	Carelli et al. (2015)
		Intron 19	c.1870 + 1G > T	p.(?)				
13	C-het	Intron 27	c.2779-2A > C	p.(?)	AR	Behr syndrome	Nystagmus	Rubegni et al. (2017)
		Exon 28	c.2809C > T	p.(Arg937Cys)			Mental retardation	
14	C-het	Exon7	c.740G > A	p.(Arg247His)	AD	OA plus syndrome	–	Yu-Wai-Man et al. (2010b)
		Exon 10	c.1019A > G	p.(Gln340Arg)				
15	C-het	Exon 8	c.800_801del	p.(Lys267Argfs*4)	AD	OA plus syndrome	–	Yu-Wai-Man et al. (2010b)
		Exon 19	c.1807G > A	p.(Val603Ile)				
16	C-het	Exon 14	c.1311A > G	p.(Ile437Met)	AD	OA plus syndrome	Nystagmus	Amati-Bonneau et al. (2009)
		Exon 29	c.2873_2876del	p.(Val958Glyfs*3)				
17	C-het	Exon 14	c.1311A > G	p.(Ile437Met)	AD	OA plus syndrome	Nystagmus	Nasca et al. (2017)
		Exon 2	c.190_194del	p.(Ser64Aspfs*7)				
18	C-het	Exon 14	c.1311A > G	p.(Ile437Met)	AD	OA plus syndrome	Ptosis	Nasca et al. (2017)
		Exon 29	c.2962G > T	p.(Val988Phe)				
19	C-het	Exon 14	c.1311A > G	p.(Ile437Met)	AD	OA plus syndrome	–	Bonifert et al. (2014)
		Exon 14	c.1316_1317insA	p.(Asn440Lysfs*14)				
20	C-het	Exon 14	c.1311A > G	p.(Ile437Met)	AD	OA plus syndrome	–	Bonifert et al. (2014)
		Exon 26	c.2635C > T	p.(Arg879*)				

Table 3 (continued)

No	Status	Position	Nucleotide change	Protein	Inheritance	Phenotype	Other findings	References
21	C-het	Exon 14	c.1311A > G	p.(Ile437Met)	AD	OA plus syndrome	–	Bonifert et al. (2014)
		Exon 19	c.1834C > T	p.(Arg612*)				
22	C-het	Exon 14	c.1311A > G	p.(Ile437Met)	AD	OA plus syndrome	–	Bonifert et al. (2014)
		Exon 17	c.1624G > A	p.(Glu542Lys)				
23	C-het	Exon 8	c.826G > A	p.(Glu276Lys)	AD	OA plus syndrome	Epilepsy	Liao et al. (2017)
		Exon 29	c.2873_2876del	p.(Val958Glyfs*3)				
24	C-het	Exon 25	c.2518del	p.(Gln840Serfs*15)	AD	OA plus syndrome	–	Liao et al. (2017)
		Exon 30	c.3034C > T	p.(His1012Tyr)				
25	Hom	Exon 19	c.1601 T > G	p.(Leu534Arg)	AD	OA plus syndrome	Cardiomyopathy	Spiegel et al. (2016)
26	C-het	Exon 14	c.1311A > G	p.(Ile437Met)	AD	OA plus syndrome	–	Zerem et al. (2019)
		Exon 22	c.2128_2129dup	p.(Lys711Serfs*16)				

Hom homozygous, *C-het* compound heterozygous, *AD* autosomal dominant, *AR* autosomal recessive, *OA* optic atrophy, *ERG* electroretinogram, *LCA* Leber congenital amaurosis, – not applicable
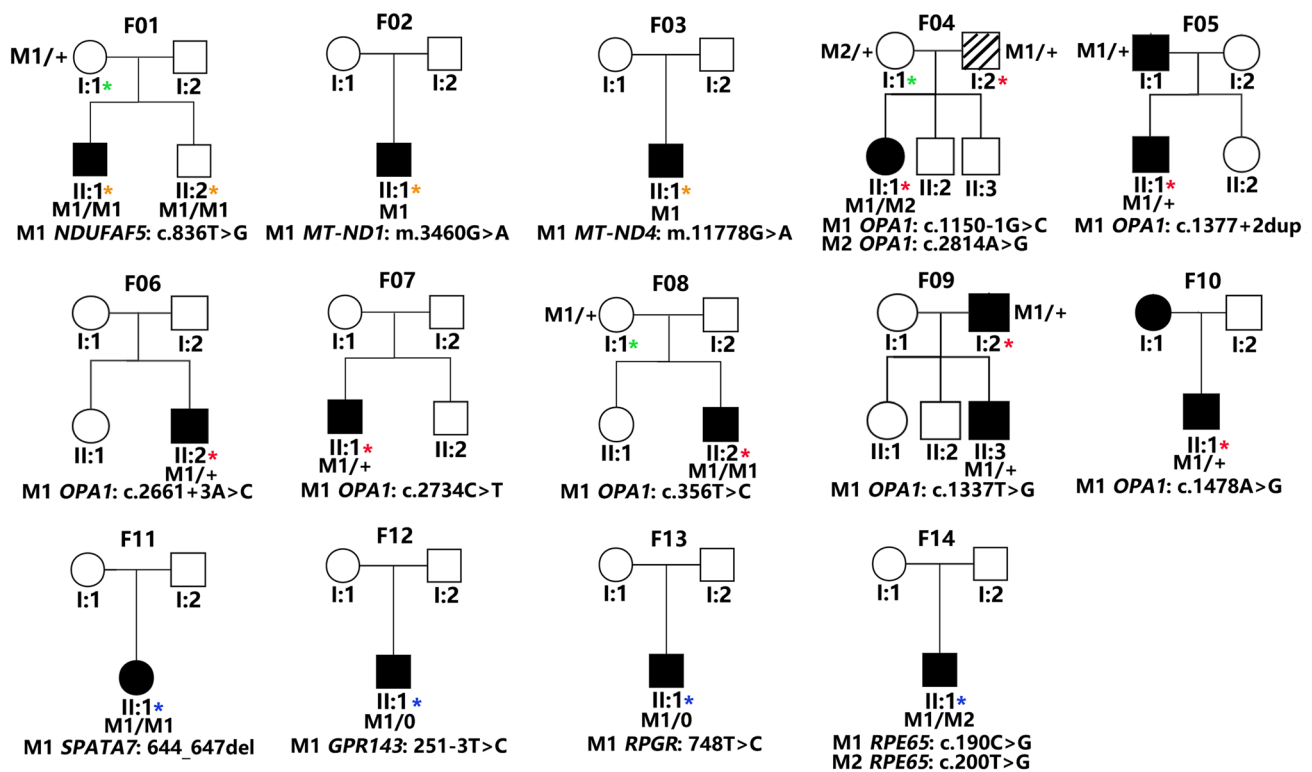
Fig. 4 The pedigrees of the individuals recruited for OCR measurements. The individuals in this study were marked with *. The individuals with pathogenic *NDUFAF5, MT-ND1* and *MT-ND4* variants were demonstrated in orange, those with pathogenic *OPA1* variants were in red, asymptomatic carriers in green and others without mitochondria related pathogenic variants in blue

compared with those for the group IV patients, while those for the group II patients were 63.2%, 59.3%, and 43.6%, respectively, compared with those for the group IV patients.

Group III patients showed no significant changes in basal respiration ($P > 0.05$) or ATP production ($P > 0.05$) but an approximate 67% level of spare respiratory capacity

Fig. 5 Phase-contrast light micrograph of human urine cells. The cell colonies could be observed 5–7 days after isolation (**a**). All the primary cells reached an 80–90% confluence within 3 weeks (**b**, **c**), and were passaged and used for the subsequent study (**d**). Scale bar 500 μm
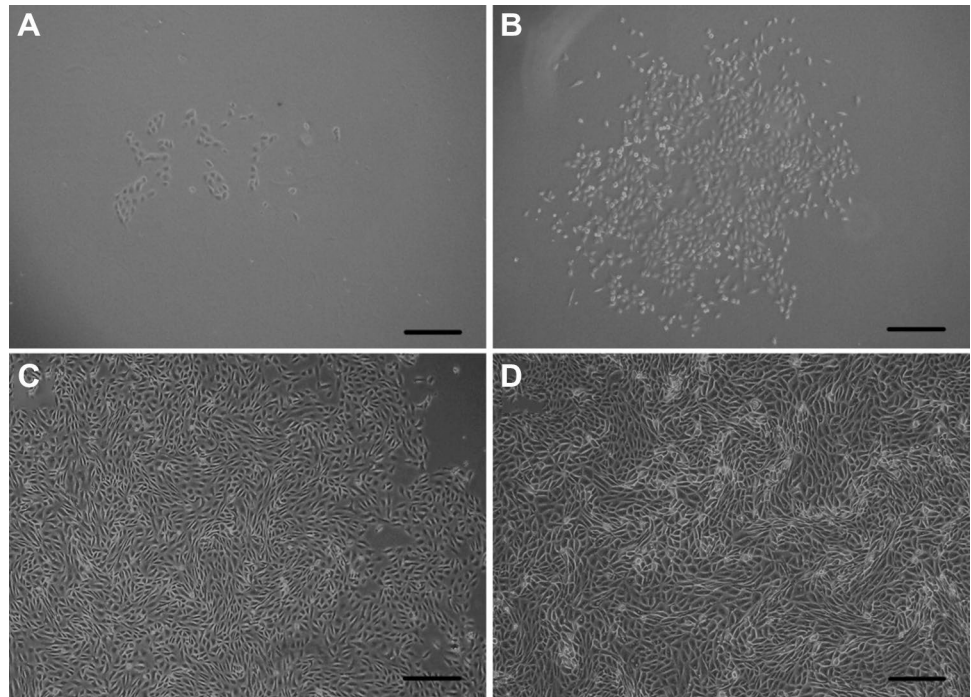
compared to that of the group IV patients. The five patients with other retinal degenerative conditions had OCR levels similar to those of the normal control for all the measurements. No significant differences were detected among different individuals within each group (Fig. 6c–e).

The OCR decreased in cells with pathogenic variants directly related to mitochondria. In addition, these measurements were related to the type and status of the variant in *OPA1* since the cells with pathogenic missense variants demonstrated higher values than those with truncation variants or biallelic variants. In addition, the homozygous missense variant in *OPA1* was associated with the same OCR as those with truncation variants in *OPA1* and with variants in *NDUFAF5*, *MT-ND1*, or *MT-ND4*. The benign variants were related to impaired spare respiratory capacity under stress but not with basal respiration or ATP production.

Discussion

In this study, 94 rare *OPA1* variants were detected in 7092 probands with hereditary eye diseases and control groups by WES or TES. 33 pathogenic variants including 8 novel variants were discovered in 36 families while 34 manifested as ADOA. According to the ACMG standards and previous studies, the pathogenicity of truncation variants that lead to loss-of-function was relatively definite (Richards et al. 2015). Therefore, the difficulty in evaluating the pathogenicity of *OPA1* variants lay mainly in that of missense variants. Two integrative bioinformatic prediction tools of

CADD and REVEL as well as conventional online tools of Polyphen-2, SIFT and PROVEAN were applied for these missense variants. According to our analysis, the results indicated that the folllowing: (1) the heterozygous missense variants beyond the GTPase domain with the CADD and REVEL scores lower than the cut-off scores of 90% in gnomAD were likely benign; (2) the heterozygous variants in exon 7 (exon 5b referred to isoform 1) might be tolerated; (3) the splicing variants in intron 4 might be benign; (4) the frameshift variants at the 3′ terminus might be pathogenic with untruncated OPA1 protein; (5) some variants might be tolerated in heterozygous status but damaging in biallelic status, which was confirmed by the measurement of OCR in urine cells; (6) the types of variants seemed to have no correlation with the extent of vision impairment; (7) optic atrophy plus syndrome was more common in patients with pathogenic missense variants than in those with pathogenic truncation variants.

It was not uncommon to find an *OPA1* variant in patients with hereditary eye disease other than ADOA, which proposed the requirement to assess the pathogenicity of *OPA1* variants and to comprehend the genotype–phenotype correlation of *OPA1* variants. In some previous studies, although the variants were detected in patients with hereditary eye diseases, no family history was mentioned, and these variants were predicted benign by multiple online tools. Therefore, their pathogenicity should be reevaluated cautiously. There was a frameshift insertion in exon 5 (c.577_578dup, exon 4b referred to isoform 1) in gnomAD of normal control, and no reports of adverse events so far in human because
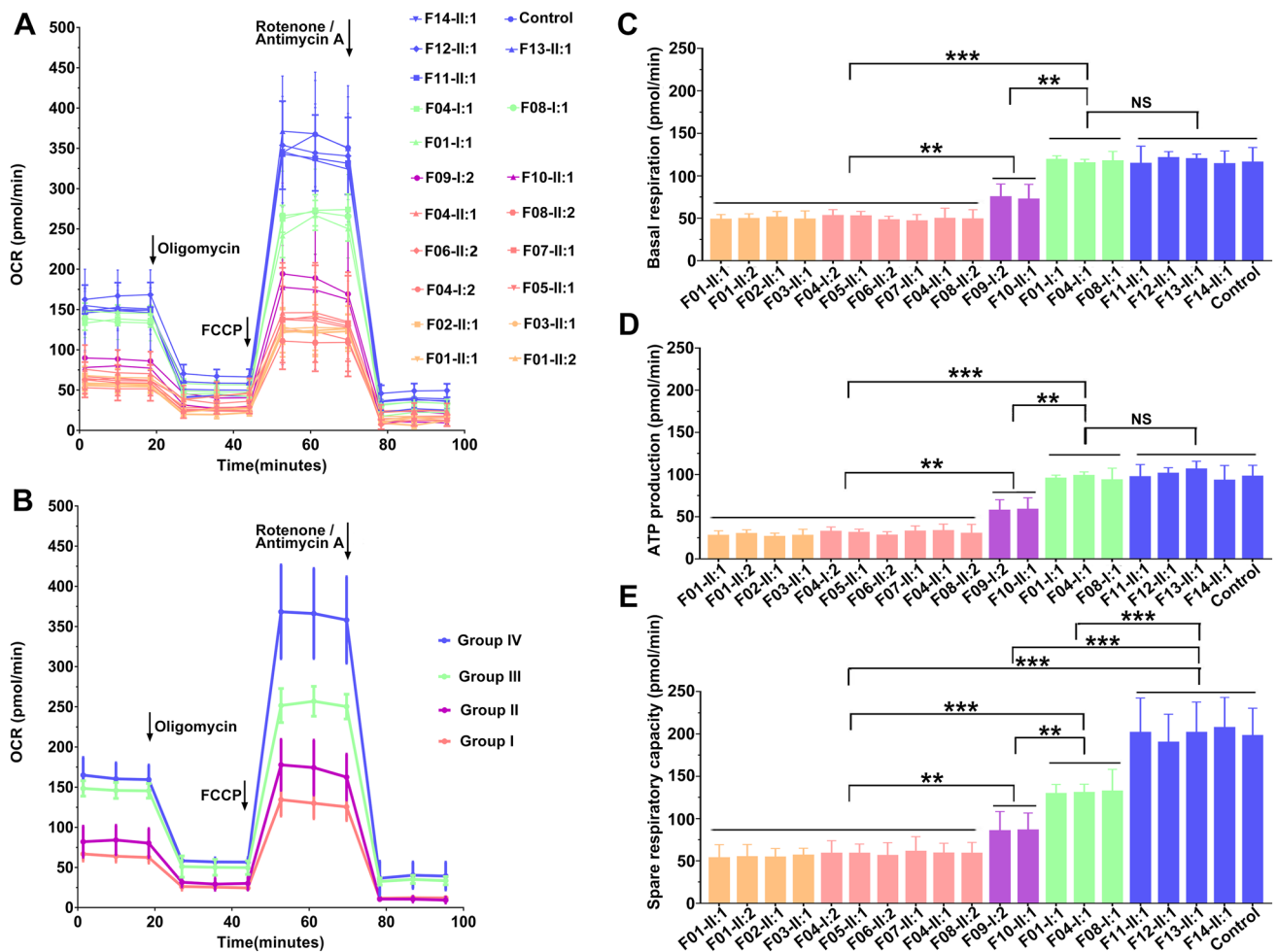
Fig. 6 The OCR measurements of the individuals in this study. The measurements were initiated every 8 min, thrice in each stage, 5 wells for each individual. **a** The OCR measurement of each individual. **b** The OCR measurement of each group demonstrated in mean values. **c** Basal respiration of each individual. **d** ATP production of each individual. **e** Spare respiratory capacity of each individual

of variants in this exon. More follow-up studies would be expected to understand their significance. Furthermore, two missense variants in exon 7 (exon 5b referred to isoform 1) detected in former studies might be benign and further investigations of their significance in ADOA were expected. As with the variant of c.740G > A, it was detected in patients of ADOA with biallelic variants (Yu-Wai-Man et al. 2010b). This variant alone might not be pathogenic. And the variant of c.768C > G was detected in a patient who had recovered vision with age which showed inconsistent with usual course of ADOA (Cornille et al. 2008). The possible reason for this might be that the isoforms of OPA1 proteins with exon 7 (exon 5b referred to isoform 1) play a less important part in retina (Delettre et al. 2001). Notably, there were two non-ADOA probands with the splicing variant of c.556 + 2 T > G in intron 4 in this study. It was considered pathogenic in one study (Zhang et al. 2017), but there were no follow-up cases reported or included in the *OPA1* database. According to

the latest researches, some soluble OPA1 isoforms without exon 1 to exon 4 were found in the mitochondrial intermembrane space (Del Dotto et al. 2017), so some heterozygous splicing variants in intron 1 to intron 4 that lead to exon skipping, shortening with a minor length change in protein might be tolerated, their impact and pathogenicity should be reevaluated.

The pathogenic variants in *OPA1* were first reported in ADOA patients by Alexander and Delettre at the same time (Alexander et al. 2000; Delettre et al. 2000). In subsequent studies, it was noticed that ADOA patients might be combined with other neuromuscular symptoms, called optic atrophy plus syndrome which was more common in patients with pathogenic missense variants (Amati-Bonneau et al. 2009). It was presumed to be the consequence of dominant-negative-effect. In addition, the patients with the same variant of c.2873_2876del manifested different degrees of nonsense-mediated mRNA decay, which indicated the involvement of

other regulatory factors (Delettre et al. 2001). This might help to explain the phenotypic heterogeneity in patients with the same variant. Several pathogenic frameshift variants in the penultimate exon of exon 30 in the last 50 base pairs at the 3′ terminus were detected both in this study and previous studies. These variants were predicted to resist to nonsense-mediated mRNA decay and have a high likelihood of an expressed protein in almost normal length (Lejeune and Maquat 2005; Hug et al. 2016). Therefore, the pathogenicity might be different from other truncation variants which involved in haploinsufficiency.

In this study, five patients with biallelic *OPA1* variants were found. The missense variants they carried were found in asymptomatic family members and were classified as benign based on our criteria. However, we found that patients with biallelic variants had an earlier age of onset and lower vision acuity than members of the same family with truncation variants. The patient with homozygous variant exhibited optic atrophy while his heterozygous family members were asymptomatic. It was unclear what role these variants played in the occurrence of the disease. But these variations seemed to show synergistic or superimposed effects in clinical phenotypes. At the same time, when measuring the OCR of urine cells, the values of cells with biallelic variants were lower than that of cells with heterozygous variants from their family members. Further investigations were needed clarify the underlying mechanism.

In conclusion, the pathogenic variants in *OPA1* causing ADOA were mainly truncation variants and missense variants in the GTPase domain both in this study and previous studies. Furthermore, some variants might be benign according to our analysis, although they were considered pathogenic in previous studies especially the missense variants beyond the GTPase domain with low CADD and REVEL scores or some splicing variants in intron 1 to intron 4. In addition, the penetrance of the missense variants was higher than that of truncation variants, and the missense variants in patients with biallelic variants seemed to play an important part in the occurrence of the disease. Finally, measuring the oxygen consumption rates in urine cells was a specific test to evaluate the effects of variants on mitochondrial function. It could be used as a method to evaluate the pathogenicity of some *OPA1* variants. Our detailed and systematical evaluation might be of assistance not only for *OPA1* alone but also for some other genes in autosomal dominant inheritance. And a comprehensive variant evaluation for a specific gene is valuable and indispensable especially when genetic tests are increasingly important in the clinical applications.

Supplementary Information The online version contains supplementary material available at https://doi.org/10.1007/s00438-021-01783-0.

Declarations

Conflict of interest The authors declare no conflict of interest.

Ethical approval All procedures in this study conformed to the tenets of the Helsinki Declaration, and was approved by the ZOC institutional review board.

Informed consent Informed consent was obtained from all participants or their guardians prior to the collection of clinical data, venous blood and urine samples.

References

Alexander C, Votruba M, Pesch UE, Thiselton DL, Mayer S, Moore A, Rodriguez M, Kellner U, Leo-Kottler B, Auburger G, Bhattacharya SS, Wissinger B (2000) OPA1, encoding a dynamin-related GTPase, is mutated in autosomal dominant optic atrophy linked to chromosome 3q28. Nat Genet 26:211–215

Almind GJ, Ek J, Rosenberg T, Eiberg H, Larsen M, Lucamp L, Brondum-Nielsen K, Gronskov K (2012) Dominant optic atrophy in Denmark—report of 15 novel mutations in OPA1, using a strategy with a detection rate of 90%. BMC Med Genet 13:65

Amati-Bonneau P, Milea D, Bonneau D, Chevrollier A, Ferre M, Guillet V, Gueguen N, Loiseau D, de Crescenzo MA, Verny C, Procaccio V, Lenaers G, Reynier P (2009) OPA1-associated disorders: phenotypes and pathophysiology. Int J Biochem Cell Biol 41:1855–1865

Bonifert T, Karle KN, Tonagel F, Batra M, Wilhelm C, Theurer Y, Schoenfeld C, Kluba T, Kamenisch Y, Carelli V, Wolf J, Gonzalez MA, Speziani F, Schule R, Zuchner S, Schols L, Wissinger B, Synofzik M (2014) Pure and syndromic optic atrophy explained by deep intronic OPA1 mutations and an intralocus modifier. Brain 137:2164–2177

Carelli V, Sabatelli M, Carrozzo R, Rizza T, Schimpf S, Wissinger B, Zanna C, Rugolo M, La Morgia C, Caporali L, Carbonelli M, Barboni P, Tonon C, Lodi R, Bertini E (2015) 'Behr syndrome' with OPA1 compound heterozygote mutations. Brain 138:e321

Chen Y, Jia X, Wang P, Xiao X, Li S, Guo X, Zhang Q (2013) Mutation survey of the optic atrophy 1 gene in 193 Chinese families with suspected hereditary optic neuropathy. Mol Vis 19:292–302

Chen J, Xu K, Zhang X, Jiang F, Liu L, Dong B, Ren Y, Li Y (2014) Mutation screening of mitochondrial DNA as well as OPA1 and OPA3 in a Chinese cohort with suspected hereditary optic atrophy. Investig Ophthalmol Vis Sci 55:6987–6995

Cohn AC, Toomes C, Potter C, Towns KV, Hewitt AW, Inglehearn CF, Craig JE, Mackey DA (2007) Autosomal dominant optic atrophy: penetrance and expressivity in patients with OPA1 mutations. Am J Ophthalmol 143:656–662

Cornille K, Milea D, Amati-Bonneau P, Procaccio V, Zazoun L, Guillet V, El Achouri G, Delettre C, Gueguen N, Loiseau D, Muller A, Ferre M, Chevrollier A, Wallace DC, Bonneau D, Hamel C, Reynier P, Lenaers G (2008) Reversible optic neuropathy with OPA1 exon 5b mutation. Ann Neurol 63:667–671

Dadgar S, Hagens O, Dadgar SR, Haghighi EN, Schimpf S, Wissinger B, Garshasbi M (2006) Structural model of the OPA1 GTPase domain may explain the molecular consequences of a novel mutation in a family with autosomal dominant optic atrophy. Exp Eye Res 83:702–706

Del Dotto V, Mishra P, Vidoni S, Fogazza M, Maresca A, Caporali L, McCaffery JM, Cappelletti M, Baruffini E, Lenaers G, Chan D, Rugolo M, Carelli V, Zanna C (2017) OPA1 isoforms in the hierarchical organization of mitochondrial functions. Cell Rep 19:2557–2571

Delettre C, Lenaers G, Griffoin JM, Gigarel N, Lorenzo C, Belenguer P, Pelloquin L, Grosgeorge J, Turc-Carel C, Perret E, Astarie-Dequeker C, Lasquellec L, Arnaud B, Ducommun B, Kaplan J, Hamel CP (2000) Nuclear gene OPA1, encoding a mitochondrial dynamin-related protein, is mutated in dominant optic atrophy. Nat Genet 26:207–210

Delettre C, Griffoin JM, Kaplan J, Dollfus H, Lorenz B, Faivre L, Lenaers G, Belenguer P, Hamel CP (2001) Mutation spectrum and splicing variants in the OPA1 gene. Hum Genet 109:584–591

den Dunnen JT, Dalgleish R, Maglott DR, Hart RK, Greenblatt MS, McGowan-Jordan J, Roux AF, Smith T, Antonarakis SE, Taschner PE (2016) HGVS recommendations for the description of sequence variants: 2016 update. Hum Mutat 37:564–569

Divakaruni AS, Paradyse A, Ferrick DA, Murphy AN, Jastroch M (2014) Analysis and interpretation of microplate-based oxygen consumption and pH data. Methods Enzymol 547:309–354

Dorrenhaus A, Muller JI, Golka K, Jedrusik P, Schulze H, Follmann W (2000) Cultures of exfoliated epithelial cells from different locations of the human urinary tract and the renal tubular system. Arch Toxicol 74:618–626

Ferre M, Bonneau D, Milea D, Chevrollier A, Verny C, Dollfus H, Ayuso C, Defoort S, Vignal C, Zanlonghi X, Charlin JF, Kaplan J, Odent S, Hamel CP, Procaccio V, Reynier P, Amati-Bonneau P (2009) Molecular screening of 980 cases of suspected hereditary optic neuropathy with a report on 77 novel OPA1 mutations. Hum Mutat 30:E692-705

Fokkema IF, Taschner PE, Schaafsma GC, Celli J, Laros JF, den Dunnen JT (2011) LOVD vol 2.0: the next generation in gene variant databases. Hum Mutat 32:557–563

Frezza C, Cipolat S, Martins de Brito O, Micaroni M, Beznoussenko GV, Rudka T, Bartoli D, Polishuck RS, Danial NN, De Strooper B, Scorrano L (2006) OPA1 controls apoptotic cristae remodeling independently from mitochondrial fusion. Cell 126:177–189

Hug N, Longman D, Caceres JF (2016) Mechanism and regulation of the nonsense-mediated decay pathway. Nucleic Acids Res 44:1483–1495

Jiang D, Li J, Xiao X, Li S, Jia X, Sun W, Guo X, Zhang Q (2014) Detection of mutations in LRPAP1, CTSH, LEPREL1, ZNF644, SLC39A5, and SCO2 in 298 families with early-onset high myopia by exome sequencing. Investig Ophthalmol Vis Sci 56:339–345

Le Roux B, Lenaers G, Zanlonghi X, Amati-Bonneau P, Chabrun F, Foulonneau T, Caignard A, Leruez S, Gohier P, Procaccio V, Milea D, den Dunnen JT, Reynier P, Ferré M (2019) OPA1: 516 unique variants and 831 patients registered in an updated centralized Variome database. Orphanet J Rare Dis 14:214

Lee J, Jung SC, Hong YB, Yoo JH, Koo H, Lee JH, Hong HD, Kim SB, Chung KW, Choi BO (2016) Recessive optic atrophy, sensorimotor neuropathy and cataract associated with novel compound heterozygous mutations in OPA1. Mol Med Rep 14:33–40

Lejeune F, Maquat LE (2005) Mechanistic links between nonsense-mediated mRNA decay and pre-mRNA splicing in mammalian cells. Curr Opin Cell Biol 17:309–315

Li Y, Li J, Jia X, Xiao X, Li S, Guo X (2017) Genetic and clinical analyses of DOA and LHON in 304 Chinese patients with suspected childhood-onset hereditary optic neuropathy. PLoS ONE 12:e0170090

Li S, Xiao X, Yi Z, Sun W, Wang P, Zhang Q (2020) RPE65 mutation frequency and phenotypic variation according to exome sequencing in a tertiary centre for genetic eye diseases in China. Acta Ophthalmol 98:e181–e190

Liao C, Ashley N, Diot A, Morten K, Phadwal K, Williams A, Fearnley I, Rosser L, Lowndes J, Fratter C, Ferguson DJ, Vay L, Quaghebeur G, Moroni I, Bianchi S, Lamperti C, Downes SM, Sitarz KS, Flannery PJ, Carver J, Dombi E, East D, Laura M, Reilly MM, Mortiboys H, Prevo R, Campanella M, Daniels MJ, Zeviani M, Yu-Wai-Man P, Simon AK, Votruba M, Poulton J (2017) Dysregulated mitophagy and mitochondrial organization in optic atrophy due to OPA1 mutations. Neurology 88:131–142

Liu R, Chan DC (2017) OPA1 and cardiolipin team up for mitochondrial fusion. Nat Cell Biol 19:760–762

Morny EK, Margrain TH, Binns AM, Votruba M (2015) Electrophysiological ON and OFF responses in autosomal dominant optic atrophy. Investig Ophthalmol Vis Sci 56:7629–7637

Nasca A, Rizza T, Doimo M, Legati A, Ciolfi A, Diodato D, Calderan C, Carrara G, Lamantea E, Aiello C, Di Nottia M, Niceta M, Lamperti C, Ardissone A, Bianchi-Marzoli S, Iarossi G, Bertini E, Moroni I, Tartaglia M, Salviati L, Carrozzo R, Ghezzi D (2017) Not only dominant, not only optic atrophy: expanding the clinical spectrum associated with OPA1 mutations. Orphanet J Rare Dis 12:89

Nochez Y, Arsene S, Gueguen N, Chevrollier A, Ferre M, Guillet V, Desquiret V, Toutain A, Bonneau D, Procaccio V, Amati-Bonneau P, Pisella PJ, Reynier P (2009) Acute and late-onset optic atrophy due to a novel OPA1 mutation leading to a mitochondrial coupling defect. Mol Vis 15:598–608

Olichon A, Emorine LJ, Descoins E, Pelloquin L, Brichese L, Gas N, Guillou E, Delettre C, Valette A, Hamel CP, Ducommun B, Lenaers G, Belenguer P (2002) The human dynamin-related protein OPA1 is anchored to the mitochondrial inner membrane facing the inter-membrane space. FEBS Lett 523:171–176

Pesch UE, Leo-Kottler B, Mayer S, Jurklies B, Kellner U, Apfelstedt-Sylla E, Zrenner E, Alexander C, Wissinger B (2001) OPA1 mutations in patients with autosomal dominant optic atrophy and evidence for semi-dominant inheritance. Hum Mol Genet 10:1359–1368

Richards S, Aziz N, Bale S, Bick D, Das S, Gastier-Foster J, Grody WW, Hegde M, Lyon E, Spector E, Voelkerding K, Rehm HL (2015) Standards and guidelines for the interpretation of sequence variants: a joint consensus recommendation of the American College of Medical Genetics and Genomics and the Association for Molecular Pathology. Genet Med 17:405–424

Rubegni A, Pisano T, Bacci G, Tessa A, Battini R, Procopio E, Giglio S, Pasquariello R, Santorelli FM, Guerrini R, Nesti C (2017) Leigh-like neuroimaging features associated with new biallelic mutations in OPA1. Eur J Paediatr Neurol 21:671–677

Schimpf S, Fuhrmann N, Schaich S, Wissinger B (2008) Comprehensive cDNA study and quantitative transcript analysis of mutant OPA1 transcripts containing premature termination codons. Hum Mutat 29:106–112

Spiegel R, Saada A, Flannery PJ, Burte F, Soiferman D, Khayat M, Eisner V, Vladovski E, Taylor RW, Bindoff LA, Shaag A, Mandel H, Schuler-Furman O, Shalev SA, Elpeleg O, Yu-Wai-Man P (2016) Fatal infantile mitochondrial encephalomyopathy, hypertrophic cardiomyopathy and optic atrophy associated with a homozygous OPA1 mutation. J Med Genet 53:127–131

Sun W, Huang L, Xu Y, Xiao X, Li S, Jia X, Gao B, Wang P, Guo X, Zhang Q (2015) Exome sequencing on 298 probands with early-onset high myopia: approximately one-fourth show potential pathogenic mutations in RetNet genes. Investig Ophthalmol Vis Sci 56:8365–8372

Thiselton DL, Alexander C, Taanman JW, Brooks S, Rosenberg T, Eiberg H, Andreasson S, Van Regemorter N, Munier FL, Moore AT, Bhattacharya SS, Votruba M (2002) A comprehensive survey of mutations in the OPA1 gene in patients with autosomal dominant optic atrophy. Investig Ophthalmol Vis Sci 43:1715–1724

Varanita T, Soriano ME, Romanello V, Zaglia T, Quintana-Cabrera R, Semenzato M, Menabo R, Costa V, Civiletto G, Pesce P, Viscomi C, Zeviani M, Di Lisa F, Mongillo M, Sandri M, Scorrano L (2015) The OPA1-dependent mitochondrial cristae remodeling pathway controls atrophic, apoptotic, and ischemic tissue damage. Cell Metab 21:834–844

Wang P, Li S, Sun W, Xiao X, Jia X, Liu M, Xu L, Long Y, Zhang Q (2019) An ophthalmic targeted exome sequencing panel as a powerful tool to identify causative mutations in patients suspected of hereditary eye diseases. Transl Vis Sci Technol 8:21

Xu Y, Guan L, Xiao X, Zhang J, Li S, Jiang H, Jia X, Yang J, Guo X, Yin Y, Wang J, Zhang Q (2015) Mutation analysis in 129 genes associated with other forms of retinal dystrophy in 157 families with retinitis pigmentosa based on exome sequencing. Mol Vis 21:477–486

Xu Y, Xiao X, Li S, Jia X, Xin W, Wang P, Sun W, Huang L, Guo X, Zhang Q (2016) Molecular genetics of Leber congenital amaurosis in Chinese: new data from 66 probands and mutation overview of 159 probands. Exp Eye Res 149:93–99

Yoshida S, Yamaji Y, Yoshida A, Kuwahara R, Fujisawa K, Ishibashi T (2006) Prognostic DNA testing and counselling for dominant optic atrophy due to a novel OPA1 mutation. Can J Ophthalmol 41:614–616

Yu-Wai-Man P, Griffiths PG, Burke A, Sellar PW, Clarke MP, Gnanaraj L, Ah-Kine D, Hudson G, Czermin B, Taylor RW, Horvath R, Chinnery PF (2010a) The prevalence and natural history of dominant optic atrophy due to OPA1 mutations. Ophthalmology 117(1538–1546):1546.e1531

Yu-Wai-Man P, Griffiths PG, Gorman GS, Lourenco CM, Wright AF, Auer-Grumbach M, Toscano A, Musumeci O, Valentino ML, Caporali L, Lamperti C, Tallaksen CM, Duffey P, Miller J, Whittaker RG, Baker MR, Jackson MJ, Clarke MP, Dhillon B, Czermin B, Stewart JD, Hudson G, Reynier P, Bonneau D, Marques W Jr, Lenaers G, McFarland R, Taylor RW, Turnbull DM, Votruba M, Zeviani M, Carelli V, Bindoff LA, Horvath R, Amati-Bonneau P, Chinnery PF (2010b) Multi-system neurological disease is common in patients with OPA1 mutations. Brain 133:771–786

Zanna C, Ghelli A, Porcelli AM, Karbowski M, Youle RJ, Schimpf S, Wissinger B, Pinti M, Cossarizza A, Vidoni S, Valentino ML, Rugolo M, Carelli V (2008) OPA1 mutations associated with dominant optic atrophy impair oxidative phosphorylation and mitochondrial fusion. Brain 131:352–367

Zerem A, Yosovich K, Rappaport YC, Libzon S, Blumkin L, Ben-Sira L, Lev D, Lerman-Sagie T (2019) Metabolic stroke in a patient with bi-allelic OPA1 mutations. Metab Brain Dis 34:1043–1048

Zhang AM, Bi R, Hu QX, Fan Y, Zhang Q, Yao YG (2017) The OPA1 gene mutations are frequent in Han Chinese patients with suspected optic neuropathy. Mol Neurobiol 54:1622–1630

Zhou L, Xiao X, Li S, Jia X, Zhang Q (2018) Frequent mutations of RetNet genes in eoHM: further confirmation in 325 probands and comparison with late-onset high myopia based on exome sequencing. Exp Eye Res 171:76–91

Publisher's Note Springer Nature remains neutral with regard to jurisdictional claims in published maps and institutional affiliations.